Generalized Hydrodynamic Treatment of the Interplay between Restricted Transport and Catalytic Reactions in Nanoporous Materials

David M. Ackerman, Jing Wang, and James W. Evans

Phys. Rev. Lett. **108**, 228301 — Published 30 May 2012

DOI: 10.1103/PhysRevLett.108.228301

Generalized hydrodynamic treatment of the interplay between restricted transport and catalytic reaction in nanoporous materials

David M. Ackerman,[1,2] Jing Wang,[1,3] and James W. Evans[1,3,4]

[1]Ames Laboratory – USDOE, and Departments of [2]Chemistry, [3]Mathematics, and [4]Physics & Astronomy, Iowa State University, Ames, Iowa 50011

Behavior of catalytic reactions in narrow pores is controlled by a delicate interplay between fluctuations in adsorption-desorption at pore openings, restricted diffusion, and reaction. This behavior is captured by a generalized hydrodynamic formulation of appropriate reaction-diffusion equations (RDE). These RDE incorporate an unconventional description of chemical diffusion in mixed-component quasi-single-file systems based on a refined picture of tracer diffusion for finite-length pores. The RDE elucidate the non-exponential decay of the steady-state reactant concentration into the pore and the non-mean-field scaling of the reactant penetration depth.

TEXT

Anomalous tracer diffusion of a "tagged" particle in a single-file system, where particles within narrow pores cannot pass each other, was proven in the 1960's for hard-core interactions [1] and later for general interactions [2]. Often motivated by early investigations of biological transport across membranes [3,4], numerous studies have considered single-file tracer diffusion in finite open [5], periodic [6,7], or closed [8] "pores", and in other systems [9]. This type of inhibited transport has also been recognized to impact reactivity for catalysis in zeolites and other functionalized nanoporous materials [10-15]. For the latter reaction-diffusion phenomena which are of interest here, it is actually chemical diffusion [16] which controls behavior [15], and for which the connection to tracer diffusion is not well recognized. Another key aspect of these open reaction-diffusion systems is that steady-state behavior is not described by a classic Gibbs thermodynamic ensemble. In fact, a fundamental understanding of these steady-states, which depend on both the reaction kinetics and transport, remains a significant challenge [17-19].

Our specific focus is on first-order conversion reactions, $A \rightarrow B$, occurring inside a parallel array of linear nanopores of a catalytically functionalized material such as mesoporous silica. Reactants, A, enter the pore openings, diffuse to catalytic sites, convert to a product, B, with microscopic rate k, and both reactants and products can diffuse out of the pore [11-15]. Furthermore, we assume that these pores are sufficiently narrow that passing of reactant and product species is inhibited or even excluded. It was recognized that reactivity can be strongly inhibited for single-file diffusion (SFD) relative to unhindered passing [12]. The reason is that except near their ends, the pores tend to be exclusively populated by product which is not readily extruded. Thus, the pore center does not participate in the conversion $A \rightarrow B$.

Some studies have suggested that this type of behavior, even for inhibited transport, can be captured by mean-field-type treatments of reaction-diffusion [13] which predict an exponential decay of reactant concentration into the pore with penetration depth scaling like $L_p \sim k^{\zeta}$ with $\zeta = -½$ [14,15]. However, we will find fundamental short-comings in these mean-field treatments, noting that exact behavior for SFD even exhibits different scaling of L_p with $\zeta \neq -½$. A deterministic hydrodynamic treatment [20] accounting for SFD [15] can describe reaction-diffusion behavior in the regime of slowly varying concentration profiles (for long pores) even

for SFD, but this treatment completely fails to describe steady-state reactivity [15]. The reason for this failure is that steady-state behavior is controlled by the stochastic nature of adsorption and desorption of species at the pore openings. Thus, to correctly capture behavior, in this Letter, we pursue a generalized hydrodynamic formalism. This formalism requires an appropriate description of chemical diffusion in mixed-component systems, including the case of SFD, based on a relationship between chemical and tracer diffusion deriving from interacting particle systems theory. However, it also requires a refined picture of tracer diffusion for finite-length pores.

In our model for A→B conversion (Fig.1), we consider a catalytic material composed of an array of similar parallel linear nanopores. Species within any pore are localized at a linear array of cells (or sites) labeled n=1 - L traversing the pore. The cell width "a" is chosen as a~1 nm comparable to species size. To describe the surrounding fluid, we can extend the 1D lattice inside the pores to a 3D lattice outside. But the fluid is assumed well-stirred, so that cells of the 3D lattice are randomly occupied with specified probabilities, $\langle A_{out} \rangle$ and $\langle B_{out} \rangle$, corresponding to the suitably normalized external reactant and product concentrations, respectively. The total concentration, $\langle X_{out} \rangle = \langle A_{out} \rangle + \langle B_{out} \rangle = \chi$, say, is fixed, whereas $\langle B_{out} \rangle$ slowly increases from an initial value of zero during extended reaction. This slow time-scale is controlled by the fluid volume and far exceeds that for relaxation of the concentration profile within the pore.

In the simplest prescription corresponding to SFD within the pores, A and B hop to adjacent empty (E) cells at rate h per direction. We can also allow positional exchange of adjacent A and B at rate $h_{ex} = h\,P_{ex}$ to relax the strict SFD constraint, noting that exchange of adjacent particles of the same type has no effect. The passing propensity, P_{ex}, will increase with pore diameter d from $P_{ex} = 0$ below a SFD-threshold to $P_{ex} \sim 1$ for unhindered passing. Other mechanistic steps in the model are: **(i)** Impingement of external species at terminal cells $n=1$ and $n=L$ of the pore at rate $i_A = h\langle A_{out} \rangle$ ($i_B = h\langle B_{out} \rangle$) for the reactant A (product B), successful adsorption occurring if these end cells are unoccupied or empty (E); **(ii)** Attempted desorption of both A and B from terminal cells of the pore at rate h, success occurring with probability $\langle E_{out} \rangle = 1 - \langle X_{out} \rangle$ for the neighboring fluid site to be unoccupied (E_{out}); **(iii)** Conversion A → B at rate k at catalytic cells.

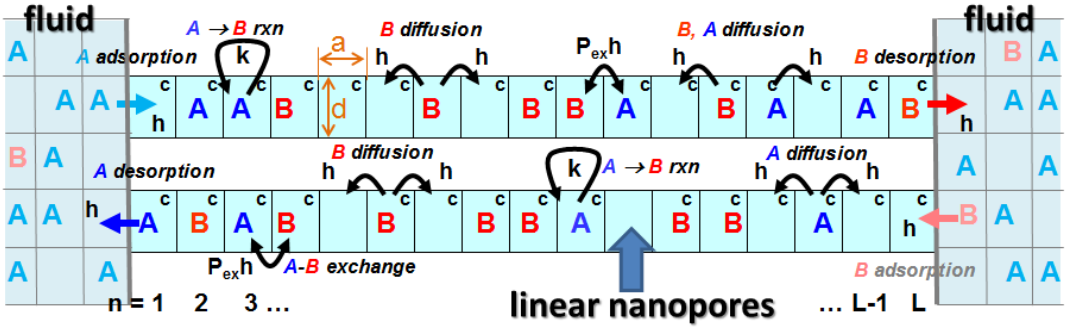

Fig.1. (Color online) Schematic of the key steps in our A→B catalytic conversion reaction model. "c" denote catalytic cells where reaction occurs at rate k. Behavior is shown in two adjacent pores which should be regarded as part of a larger array of pores.

For the above rate choice, which follows previous studies [11-15], the "species blind" dynamics for particles X = A or B corresponds to a non-reactive diffusion process. In the steady-state, cells within the pore are randomly occupied by particles, X, with probability $\langle X_{out} \rangle = \chi$ [14]. We will assess typical concentration profiles within a pore, corresponding to averaging over many pores.

Both time evolution and steady-state behavior (see Fig.2 for examples for the initial stages of reaction with $<B_{out}> \approx 0$) can be assessed precisely by Kinetic Monte Carlo (KMC) simulation.

An exact description of our discrete reaction-diffusion model is provided by hierarchical master equations for the evolution of probabilities of various configurations of subsets of cells within the pore [11,13-15]. Let $<C_n>$ denote the probability that species C = A or B is at cell n, $<C_nE_{n+1}>$ that C is at cell n and that cell n+1 is empty (E), etc. Then, the total conversion rate is $R_{tot} = k \sum_{n=c}<A_n>$ with the sum extending over all catalytic cells. Below we consider only the case of all cells catalytic (c). Then, the lowest-order equations in the hierarchy are [14,15]

$$d/dt <A_n> = -k <A_n> - \nabla J_A^{n>n+1},\ d/dt <B_n> = +k <A_n> - \nabla J_B^{n>n+1},\ \text{for } 1<n<L. \quad (1)$$

Separate equations for terminal cells reflect adsorption-desorption boundary conditions (BC's), e.g., $d/dt <A_1> = h(<A_{out}><E_1> - <E_{out}><A_1>) - k<A_1> - J_A^{1>2}$. In (1), we have defined the discrete derivative, $\nabla K_n = K_n - K_{n-1}$. The *net flux*, $J_A^{n>n+1}$, of A from site n to n+1 is given by

$$J_A^{n>n+1} = h\,[<A_nE_{n+1}> - <E_nA_{n+1}>] + h_{ex}\,[<A_nB_{n+1}> - <B_nA_{n+1}>]. \quad (2)$$

The first term gives the contribution from hopping to adjacent empty cells, and the second from exchange. The expression for the net flux, $J_B^{n>n+1}$, of B is analogous. In the special case of unhindered transport where $P_{ex} = 1$ so $h_{ex} = h$, (2) reduces exactly to $J_A^{n>n+1} = -h\ \nabla<A_n>$ [15,21].

Equations (1) couple to pair probabilities in (2). Pair probability evolution couples to that of triples, etc., producing a hierarchy. Multi-site probabilities are not simply related to single-cell probabilities due to spatial correlations. The lowest-order site-approximation, $<C_nE_{n+1}> \approx <C_n><E_{n+1}>$, etc., produces a closed set of discrete reaction-diffusion equations (RDE) for single-cell concentrations. A pair approximation factorizes triples in terms of pair and single-cell quantities generating a closed set of equations for these [13-15]. The triplet approximation factorizes quartets in terms of triplets, etc. [22]. However, these and all higher-order mean-field (MF) like truncation approximations suffer fundamental shortcomings. While accuracy increases with the order of the approximation, convergence to exact behavior can be slow. See Fig.2a.

An alternative coarse-grained description considers concentrations per unit length, $C(x=na, t) \approx a^{-1} <C_n>$, for C = A or B, smoothly varying with position x, which satisfy the continuum RDE

$$\partial/\partial t\, A(x, t) = -k\, A(x, t) - \partial/\partial x\, J_A, \qquad \partial/\partial t\, B(x, t) = +k\, A(x, t) - \partial/\partial x\, J_B. \quad (3)$$

BC's for (3) at the pore ends reflect the adsorption-desorption dynamics [15]. Description of the diffusion fluxes, J_A and J_B, is critical. Setting $X(x,t)=A(x,t)+B(x,t)$, we exploit a little-used result from interacting particle systems theory for mixtures of particles with identical dynamics [23]

$$J_A = -D(A/X)\partial X/\partial x - D_{tr}[(B/X)\partial A/\partial x - (A/X)\partial B/\partial x] \rightarrow -D_{tr}\,\partial A/\partial x \text{ for uniform } X=a^{-1}\chi, \quad (4)$$

The form of J_B is analogous. Here $D = a^2h$ is the chemical diffusion coefficient for particles X, and $D_{tr} = D\,F_{tr}$ is a tracer diffusion coefficient. The site-approximation described above implies the mean-field form $F_{tr} = 1 - \chi$ [14,15] as is evident after coarse-graining of the discrete RDE. This choice overestimates fluxes for SFD. A classic analysis of SFD for infinite systems [1] finds that $F_{tr} = 0$. The associated "hydrodynamic" RDE can describe the evolution of slowly varying profiles during filling of long pores [15]. However, this formulation which sets the diffusion

fluxes to zero and neglects fluctuations near pore openings completely fails to describe steady-state profiles [15] as shown in Fig.2a. A refined treatment setting $F_{tr} \sim 1/L$, motivated by studies of finite-sized SFD systems [3,4,6,7], does not resolve this basic shortcoming.

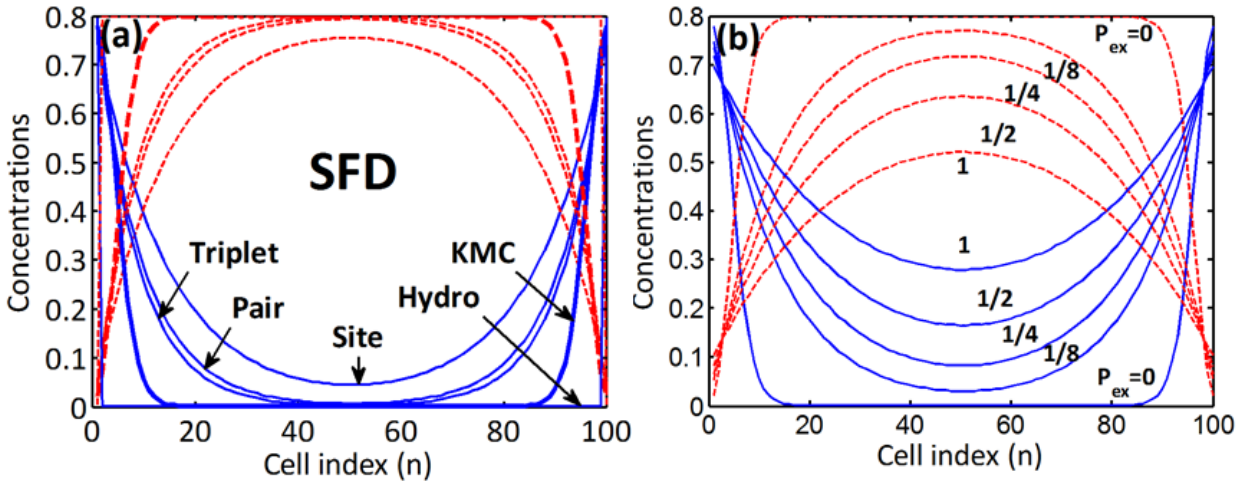

Fig.2. (Color online) Steady-state concentration profiles (A=solid, blue; B=red, dashed) for pore length $L=100$, $k=0.001$, $h=1$, and $\chi=0.8$: (a) predictions of site, pair, triplet approximations and the standard hydrodynamic treatment (hydro) versus precise KMC results for SFD ($P_{ex}=0$); (b) KMC results for restricted passing with various $P_{ex} \geq 0$.

Thus, our strategy is to develop a "generalized hydrodynamic" form for F_{tr} which captures the mesoscale fluctuations near pore openings being enhanced in these regions. A discrete form of (4) incorporating this F_{tr} then provides fluxes in (1) which are integrated to determine steady-state behavior. One strategy to determine this $F_{tr}(n)$ at cell n [24] for a pore with uniform $\langle X_n \rangle = \chi$ is based analysis of the "exit time", $t_n(\chi)$, for a tagged particle starting at this cell to reach a pore opening in the sense that its root-mean-square (rms) displacement grows to match the distance from the nearest pore opening. Specifically, we set $F_{tr}(n) = t_n(0+)/t_n(\chi)$ since diffusivity is inversely proportional to the time for the rms displacement to reach some specified value. This recovers the correct limiting value $F_{tr}(n) \to 1$ as $\chi \to 0+$. Results for $F_{tr}(n)$ in Fig.3a for SFD in finite pores reveal a central plateau of magnitude $\sim 1/L$ (consistent with [3,4,6,7]), but with significantly larger values near pore openings. Use of this variable $F_{tr}(n)$ in appropriate RDE to determine steady-state profiles yields excellent agreement with precise results from KMC simulation for SFD with L=100, in marked contrast to all other treatments. See Fig.4 for profiles with $\langle B_{out} \rangle \approx 0$ (the initial stages of the reaction), and results in Table I for the penetration depth, L_p, naturally defined as $L_p = \sum_{1 \leq n \leq L/2} \langle A_n \rangle / \langle A_1 \rangle$.

χ=0.2	k=1	k=0.1	k=0.01	k=0.001	χ=0.8	k=1	k=0.1	k=0.01	k=0.001
KMC	1.47	2.92	6.77	15.2	KMC	1.10	1.47	2.64	5.21
GHydro	1.49	3.10	7.19	15.8	GHydro	1.06	1.43	2.61	5.15
MF	1.53	3.37	9.46	27.8	MF	1.17	2.00	5.00	14.7

Table I. Comparison of reactant penetration depths, L_p (in units of 'a'), with $h=1$ and $L=100$, for KMC, generalized hydrodynamic (GHydro) and mean-field site-approximation (MF) analyses.

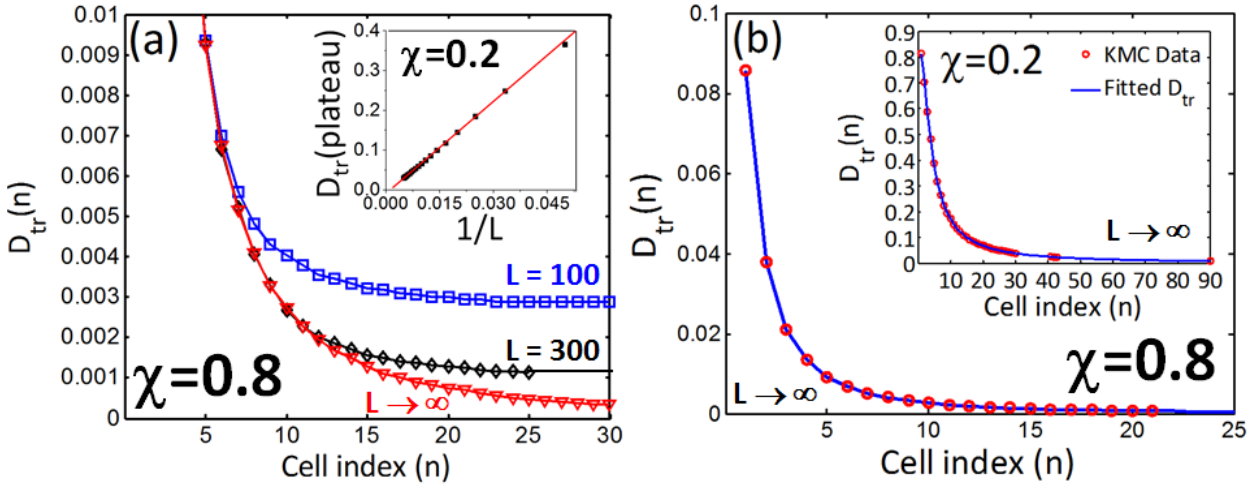

Fig.3. KMC results for $D_{tr}(n)$ [$=F_{tr}(n)$ for $a=h=1$]: (a) n-dependence for various pore lengths L for χ=0.8 (inset shows L-dependence of central plateau value of D_{tr} for χ=0.2); (b) fitting of the decay of $D_{tr}(n)$ with n for semi-infinite pore. Using the form in text, we choose $\alpha=0$, $\beta=1.543$, $\gamma=0.944$ for $\chi=0.8$ (inset: $\alpha=0.753$, $\beta=0.371$, $\gamma=0.0064$ for $\chi=0.2$).

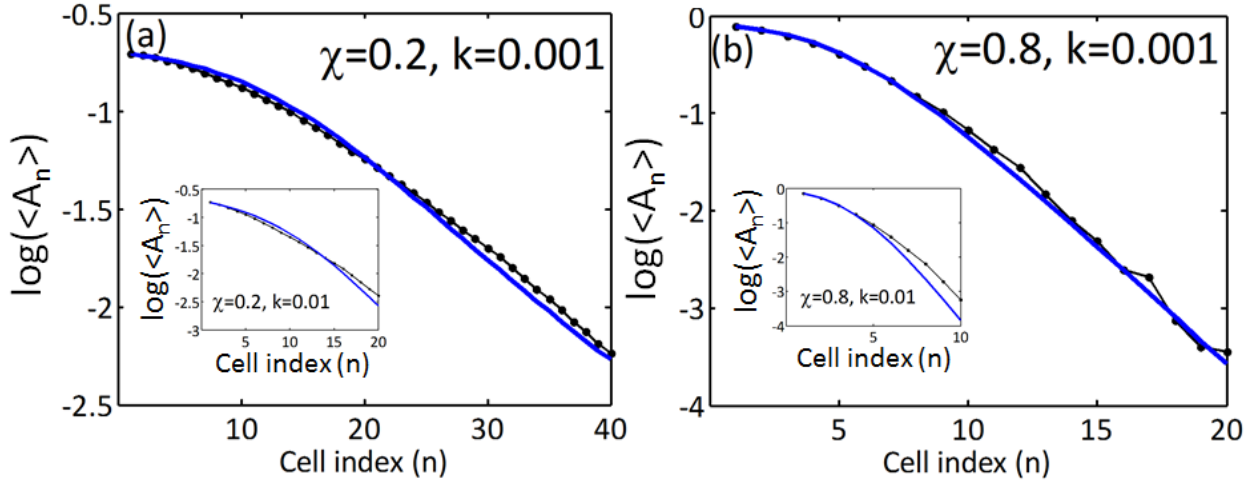

Fig.4. (Color online) Comparison of results for steady-state concentration values for $L=100$, $k=0.001$ (inset: $k=0.01$), and $h=1$ from KMC (symbols + line) with generalized hydrodynamic RDE predictions (thicker blue curves): (a) $\chi=0.2$; (b) $\chi=0.8$ (log is base 10).

Next, we turn to the fundamental issue of the form of the concentration profiles and the scaling of the penetration depth, L_p, for SFD in a semi-infinite pore with $1 \le n < \infty$. Clearly now $F_{tr}(n) \to 0$, as $n \to \infty$, but how? Deep inside the pore where classic SFD should apply, the rms displacement increases like $t^{1/4}$ [1], so one expects that $t_n(\chi>0) \sim n^4$. In contrast, $t_n(0+) \sim n^2$ for conventional diffusion. This suggests that $F_{tr}(n) \sim 1/n^2$, as $n \to \infty$. Simulation results indicate that this behavior is achieved quickly for high total concentration χ=0.8, but more slowly for low χ=0.2 which displays an intermediate regime better described by $F_{tr}(n) \sim 1/n$ scaling. Data in both cases is fit well for all n by the form $F_{tr}(n) = F_{tr}(1)(1-\alpha+\beta+\gamma)/(1-\alpha \cdot n^{1/2}+\beta \cdot n+\gamma \cdot n^2)$. See Fig.3b.

Insight into the consequences of this decay of $F_{tr}(n)$ comes from analysis of the steady-state solutions of the continuum RDE for a semi-infinite pore $x \geq 0$ using (4) with the form $F_{tr}(x) \sim 1/x^p$. One finds solutions which for small k and large L_p have the dominant form

$$A(x) \sim \exp[-(x/L_p)^q] \text{ where } q=(2+p)/2, \text{ and } L_p \sim (k/D)^{\zeta} \text{ with } \zeta = -1/(2+p). \quad (5)$$

Thus, the true asymptotic scaling exponent is $\zeta = -1/4$ (for $p=2$), but behavior mimicking $\zeta \approx -1/3$ (for $p=1$) might be seen for lower χ, both contrasting MF behavior $\zeta = -1/2$ (for $p=0$) [14,15]. These predictions are confirmed by numerical analysis of discrete generalized hydrodynamic RDE's exploiting the capability of this deterministic treatment to obtain much more precise ζ-values than possible by KMC. See Fig.5. Concentration profiles also exhibit the predicted non-exponential decay, a feature which is already indicated in the non-linear form of the log-linear plots in Fig.4 (the downward bend corresponding to an effective exponent $q>1$ due to $p>0$).

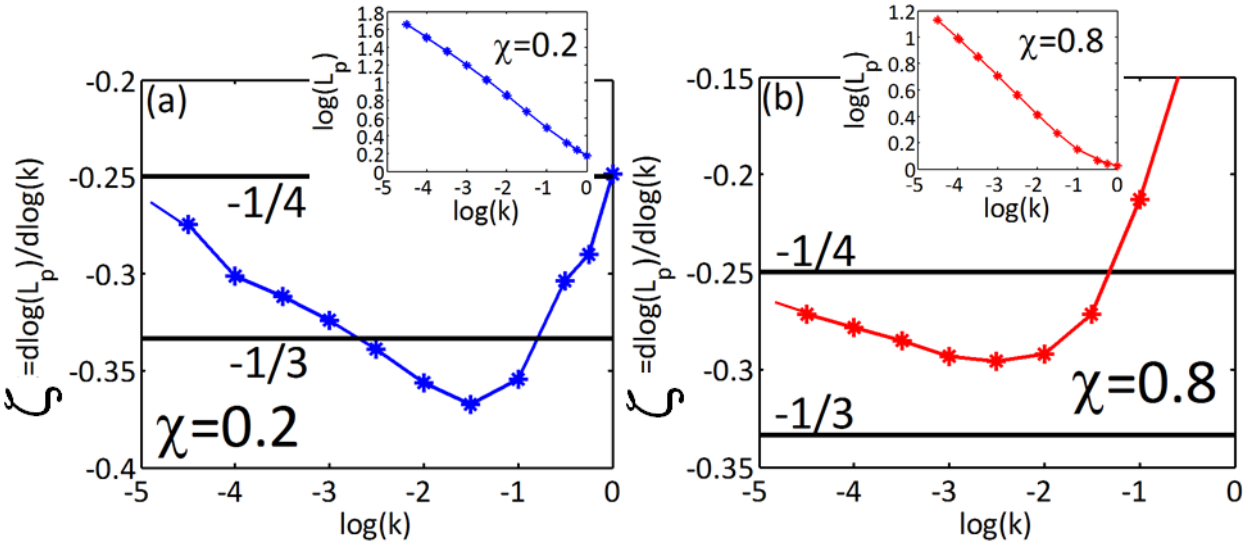

Fig.5. Predictions of generalized hydrodynamic RDE for the effective scaling exponent $\zeta = d\log(L_p)/d\log(k)$ for a semi-infinite pore: (a) $\chi=0.2$; (b) $\chi=0.8$. Upper insets: L_p versus k.

We now mention various extensions of the above analysis. All results were presented for initial stages of reaction where $\langle B_{out} \rangle \approx 0$. However, analysis is readily extended to treat arbitrary fraction of conversion $f = \langle B_{out} \rangle / \langle X_{out} \rangle$, and we find an exact linear variation with f of the total conversion rate $R_{tot}(f) = R_{tot}(0)(1-f)$ by virtue of the linearity of the RDE's and BC's. Dropping the SFD constraint, we have also analyzed $F_{tr}(n)$ which still decreases with increasing n but now retains a substantial non-zero L-independent value in the pore center corresponding to tracer diffusion with exchange in an infinite pore. The corresponding generalized hydrodynamic treatment readily recovers behavior shown in Fig.2b. The greatest challenge in developing a predictive analytic treatment is for complete or near SFD, as other cases have more MF-like behavior. One can also readily extend the analysis to treat reversible reaction A↔B using the same $F_{tr}(n)$ as determined above.

Finally, we consider more general diffusional dynamics with unequal diffusion coefficients, D_A and D_B, for A and B, respectively. Analysis for SFD reveals behavior entirely analogous to the

case of equal hop rates with penetration of reactant into the pore, but the pore center populated only by product. Again, MF treatments overestimate diffusion fluxes and fail to describe steady-state behavior. The key is to describe chemical diffusion for the mixed system (cf. [19,25]). We apply Onsager theory to determine the hydrodynamic form (corresponding to zero tracer diffusion) of $J_A = -A(A/D_A+B/D_B)^{-1} \partial X/\partial x$ for SFD, and J_B is analogous. Since the total flux, $J_X = J_A + J_B$, must vanish in the steady state, this implies that X is constant, so J_A vanishes which in turn implies that A must be absent from the pore interior due to conversion to B. This failure of the hydrodynamic description to describe reactant penetration must again be overcome by accounting for fluctuation effects at the pore openings.

In summary, the location-dependence of tracer diffusion near the openings of narrow pores is shown to control non-MF scaling of reactant penetration depth and thus reactivity for conversion reactions. Generalized hydrodynamic RDE's provide a powerful tool with which to analyze this behavior. This work is supported by the Division of Chemical Sciences – BES, USDOE. Ames Laboratory is operated for the USDOE by ISU under Contract No. DE-AC02-07CH11358.

[1] T.E. Harris, J. Appl. Prob. 2, 323 (1965).
[2] M. Kollman Phys. Rev. Lett. 90, 180602 (2003).
[3] A.L. Hodgkin and R.D. Keynes, J. Physiol. 128, 61 (1955).
[4] E.J. Harris, "Transport and accumulation in biological systems" (AP, New York, 1960).
[5] J.E. Santos and G.M. Schutz, Phys. Rev. E 64, 036107 (2001).
[6] H. van Beijeren, K.W. Kehr, and R. Kutner, Phys. Rev. B 28, 5711 (1983).
[7] A. Taloni and F. Marchesoni, Phys. Rev. E 74, 051119 (2006).
[8] L. Lizana and T. Ambjornsson, Phys. Rev. Lett. 100, 200601 (2008).
[9] E. Barkai and R. Silbey, Phys. Rev. Lett. 102, 050602 (2009).
[10] "Catalysis and adsorption in zeolites", G. Ohlman, H. Pfeifer, G. Fricke, Ed.s (Elsevier, Amsterdam, 1991).
[11] J.G. Tsikoyiannis and J.E. Wei, Chem. Eng. Sci 46, 233 (1991).
[12] C. Rodenbeck, J. Karger, and K. Hahn, J. Catal. 157, 656 (1995).
[13] M.S. Okino, R.Q. Snurr, H.H. Kung, J.E. Ochs, and M.L. Mavrovouniotis, J. Chem. Phys. 111, 2210 (1999).
[14] S.V. Nedea, A.P.J. Jansen, J.J. Lukkien, and P.A.J. Hilbers, Phys. Rev. E 65, 066701 (2002).
[15] D.M. Ackerman, J. Wang, J.H. Wendel, D.-J. Liu, M. Pruski, and J.W. Evans, J. Chem. Phys. 134, 114107 (2011).
[16] R. Krishna, J. Phys. Chem. C 113, 19765 (2009).
[17] G. Nicolis and I. Prigogine, "Self-organization in non-equilibrium systems" (Wiley, New York, 1977).
[18] J. Marro and R. Dickman, "Non-equilibrium Phase Transitions in Lattice-Gas Models" (CUP, Cambridge, 1999).
[19] J.W. Evans, D.-J. Liu, and M. Tammaro, Chaos 12, 131 (2002).
[20] H. Spohn, "Large scale dynamics of interacting particles" (Springer, Berlin, 1991).
[21] R. Kutner, Phys. Lett. 81A, 239 (1981).
[22] J.W. Evans, Rev. Mod. Phys. 75, 1281 (1993).
[23] J. Quastel, Commun. Pure Appl. Math. 45, 623 (1992).
[24] We obtain consistent results by creating steady-states with varying $\langle A_n \rangle$, but constant $\langle X_n \rangle = \chi$, and obtaining varying D_{tr} from simulation results for a discrete version of the ratio $-J_A/\partial A/\partial x$.
[25] K.W. Kehr, K. Binder, and S.M. Reulein, Phys. Rev. B 39, 4891 (1989).